Stereoselective Photooxidation of *trans*-2-Butene to Epoxide by Nitrogen Dioxide Excited with Red Light in a Cryogenic Matrix

Munetaka Nakata[†] and Heinz Frei*

Contribution from the Chemical Biodynamics Division, Lawrence Berkeley Laboratory, University of California, Berkeley, California 94720. *Received August 12, 1988*

Abstract: Reaction was induced between *trans*-2-butene and nitrogen dioxide by exciting *trans*-2-butene-NO_2 pairs, isolated in solid Ar at red, yellow, and green wavelengths ($NO_2{}^2B_2 \leftarrow \tilde{X}^2A_1$). The chemistry was monitored by FT-infrared spectroscopy, and Ar ion and cw dye lasers were used for photolysis. Products formed were 2-butene oxide + NO, the former under complete retention of stereochemistry, and an addition product that was identified by ^{18}O isotopic substitution as a butyl nitrite radical, reported here for the first time. Analysis of the photolysis-wavelength dependence of the butyl nitrite radical and *trans*-2-butene oxide (NO) growth kinetics revealed that epoxide + NO is formed along two reaction pathways. The first gives *trans*-2-butene oxide + NO and butyl nitrite radical upon absorption of a single photon by *trans*-2-butene-NO_2 pairs (one-photon path). The second path is formation of *trans*-2-butene oxide + NO by photodissociation of trapped butyl nitrite radical by a (second) red or shorter wavelength photon (two-photon path). Two alternative transients are proposed for the one-photon path, namely a hot butyl nitrite radical and an oxirane biradical, respectively. The wavelength dependence of the product branching along the one-photon path indicates that branching occurs from a vibrationally unrelaxed transient. This suggests that the observed stereochemical integrity originates from insufficient coupling of the stretching and bending vibrations of the transient with torsion around its central C-C bond on the time scale of reaction to epoxide + NO and its stabilization as butyl nitrite radical.

I. Introduction

Nitrogen dioxide excited at red or near-infrared wavelengths may be a sufficiently mild oxidant to permit product-specific oxidation of hydrocarbons and may be relevant to controlled catalytic hydrocarbon oxidation, a key problem in catalysis research. Namely, photoassisted oxidation by NO_2, where NO is a coproduct with the oxidized hydrocarbon, can be viewed as the central step of a scheme of photoassisted hydrocarbon oxidation by O_2 in which NO would play the role of a catalyst. This is possible because NO can readily be oxidized by O_2 to regenerate NO_2, hence O_2 would be the oxidant actually consumed.

We report here unusually high product specificity observed upon oxidation of an alkene by NO_2 excited at red or yellow wavelengths. Reaction was studied by exciting *trans*-2-butene-NO_2 reactant pairs, isolated in solid Ar at 12 K, with tuned radiation from a cw dye laser, and by monitoring the chemistry by FT-infrared spectroscopy. The cryogenic-matrix technique is ideally suited for the study of photoinitiated bimolecular chemistry[1-5] since the reactants of interest can be brought together as sustained pairs, and reaction can be followed in complete absence of diffusional processes that complicate elucidation of the reaction path in liquid solution or gas phase. Photolysis-wavelength dependence of the chemistry, both in terms of quantum efficiency and the course the reaction takes, can conveniently be determined by laser initiation in an inert, solid environment. Particularly useful for uncovering reaction pathways is the possibility to trap chemical intermediates. These advantages were fully exploited in the study presented here.

II. Experimental Section

Matrix suspensions of *trans*-2-butene and NO_2 were prepared by codepositing rare gas mixtures of the two reactants, NO_2/Ar and *trans*-2-butene/Ar, through separate stainless steel deposition lines onto a 12 K cooled CsI window. Deposition rates were 1 mmol/h for each mixture, over a period of 2-4 h, depending on the concentrations used. The cryostat used was a two-stage closed cycle helium refrigeration (Air Products Model CSA 202). Chemical reaction was monitored by infrared spectroscopy using an IBM-Bruker FT-IR instrument Model IR-97. Spectra were taken at a resolution of 0.5 cm^{-1}. For laser irradiation, the cold window was rotated by 90° to expose the matrix to the photolysis light entering the vacuum shroud through a quartz window. UV/vis matrix spectra were measured with a UV/vis spectrometer Perkin-Elmer Model 450.

Matrices were irradiated with light from an Ar ion laser pumped cw dye laser (Coherent Models CR-8 and 599-01, respectively), using the dyes Fluorescein (Kodak), Rhodamine 590 (Exciton), or DCM (Exciton). The dye-laser output was calibrated with an accuracy of 0.1 nm with a McPherson monochromator Model MP-1018. In a few cases, irradiation was in addition performed with the 514-nm emission line of the Ar ion laser or with all emission lines of the Ar ion laser in the 458-514-nm range ("all lines blue-green"). The laser power was monitored at the cryostat quartz window before and after each irradiation period with a Coherent power meter Model 210.

trans-2-Butene (Matheson, 95%) was used without further purification (the impurity is mostly *cis*-2-butene). Nitric oxide impurity was removed from nitrogen dioxide (Matheson, 99.5%) by adding oxygen and condensing NO_2 at 77 K. Two samples of ^{18}O-containing nitrogen dioxide were used. One sample was prepared by gas-phase oxidation of $N^{16}O$ (Matheson, 99.0%) by $^{18}O_2$ (MSD Isotopes, 98.2 atom % ^{18}O), resulting in a mixture of approximate isotopic composition of $N^{16}O_2/N^{16}O^{18}O/N^{18}O_2$ = 2/3/1 (by infrared). The second sample was obtained by oxidizing $N^{18}O$ (Icon Services, Inc., 94.5 atom % ^{18}O) by the same $^{18}O_2$ gas sample to give a gas mixture of composition $N^{16}O_2/N^{16}O^{18}O/N^{18}O_2$ = 0.1/7/93. Both mixtures were purified by trap to trap distillation (LN_2). Argon (Matheson, 99.998%) was used without further purification.

III. Results

Reactant infrared spectra and photoinduced changes of NO_2 aggregates inevitably present at the nitrogen dioxide concentrations needed here will be presented in section 1. Then, infrared spectroscopic evidence for trapping of a nitrite radical upon irradiation of *trans*-2-butene/NO_2/Ar matrices with red and yellow light will be given, and the final oxidation product will be identified (section 2). In section 3, kinetics and photolysis laser power dependence of product growth will be presented.

1. Reactant Spectra and N_xO_y Photoisomerization. The spectral range between 2000 and 400 cm^{-1} contains all infrared absorptions necessary to identify intermediate and products, hence we will confine the report of infrared spectral data to this region. Before photolysis, spectra of matrices *trans*-2-butene/NO_2/Ar = 2.5/

[†]On leave from the Faculty of Science, Hiroshima University, Hiroshima, Japan.

(1) Frei, H.; Pimentel, G. C. *J. Chem. Phys.* **1983**, *79*, 3307-3319.
(2) Frei, H. *J. Chem. Phys.* **1984**, *80*, 5616-5622.
(3) Frei, H.; Pimentel, G. C. *Annu. Rev. Phys. Chem.* **1985**, *36*, 491-524.
(4) Frei, H.; Pimentel, G. C. In *Chemistry and Physics of Matrix Isolated Species*; Andrews, L., Moskovits, M., Eds.; Elsevier: Amsterdam, 1989; p 139-165.
(5) Salama, F.; Frei, H. *J. Phys. Chem.* **1989**, *93*, 1285.

0002-7863/89/1511-5240$01.50/0

Table I. N_xO_y Absorptions in a Matrix *trans*-2-Butene/NO_2/Ar = 2.5/1/100 and Their Intensity Changes under Red-Light[a] Irradiation

frequency, cm^{-1}			
before irrad	after irrad	assignment	ref
1906 (br)	1912↓	asym N_2O_4 (P)[b]	10
1872		NO	7
	1832↓	asym N_2O_3	8
1830	1830↑	asym N_2O_4	11
1751	1754↑	sym N_2O_4 (D_{2h})	11
1732	1732↑	sym N_2O_4 (D_{2h})	11
1707 (br)	1715↑	sym N_2O_4 (D_{2d})	11
1689	1689↑	sym N_2O_3	8
1641	1644↑	asym N_2O_4	11
	1639↑	asym N_2O_4	11
1630	1631↓	asym N_2O_3	8
1572 (br)	1579↓	asym N_2O_4 (P)	10
1302	1297↓	asym N_2O_3	8
1288	1288↑	asym N_2O_4	11
1274	1275↑	sym N_2O_4 (D_{2d})	11
1257	1259↓	asym N_2O_4 (P)	10
	1256↑	sym N_2O_4 (D_{2h})	11
903	907↑	asym N_2O_4	11
	881↓	asym N_2O_4 (P)	10
875 (br)	873↑	sym N_2O_3	8
	864↓	asym N_2O_4 (P)	10
786	786↑	asym N_2O_4	11
	771↓	asym N_2O_3	8
	755↑	sym N_2O_4 (D_{2h})	11
718 (br)	718↓	asym N_2O_4 (P)	10
638	644↑	asym N_2O_4	11
578 (br)	581↓	asym N_2O_4 (P)	10
490	501↑	asym N_2O_4	11

[a] 625 nm, 270 mW cm^{-2}, 1-h irradiation. [b] P stands for precursor; this form of N_2O_4 isomerizes to asym and sym N_2O_4. The frequencies of this species, which we have previously observed in solid N_2,[10] are close to those of N_2O_4 (D') reported by St. Louis and Crawford.[11]

1/100 show bands of the reactant *trans*-2-butene (1477, 1456, 1442, 1380, 1298, 1066, 1042, 975, and 967 cm^{-1})[6] and those of NO_2 (1609, 1593 ($N^{16}O^{18}O$, natural abundance) and 749 cm^{-1}).[7] In addition, small amounts of N_2O_4 isomers are trapped in the matrix together with traces of NO and N_2O_3. At none of the matrix concentrations used could distinct infrared absorptions of *trans*-butene–NO_2 nearest neighbors be observed.

Both N_2O_4 and N_2O_3 have been reported to photoisomerize under near infrared or visible irradiation.[8,9] We have observed spectral changes associated with these interconversions at all red, yellow, and green photolysis laser wavelengths used. Absorption frequencies of N_2O_4 and N_2O_3 species found in our matrices, together with qualitative intensity changes that occurred upon irradiation with light in the range 640–570 nm are shown in Table I. As noted by other workers, positions of absorption bands of N_xO_y species produced by photolysis in the matrix differ in many cases by up to several cm^{-1} from those of species formed upon matrix deposition. Therefore, we have included in Table I the frequencies of N_xO_y molecules measured both before and after irradiation.

2. Spectra of Trapped Reaction Intermediate and Products. Irradiation of a matrix *trans*-2-butene/NO_2/Ar = 2.5/1/100 with 625-nm light at 270 mW cm^{-2} resulted in infrared band intensity changes that are exclusively due to N_xO_y isomerizations, displayed in Table I. In a more dilute matrix, e.g. *trans*-2-butene/NO_2/Ar = 2.5/1/400, these processes interfered less with our search for *trans*-butene + NO_2 chemistry since at this concentration only the most intense N_2O_4 absorptions could be observed. When irradiating *trans*-2-butene/NO_2/Ar matrices with shorter wavelength light, *trans*-2-butene absorptions began to decrease, while new bands grew in that could not be assigned to N_xO_y species. Figure 1a shows the infrared difference spectrum upon 590-nm irradiation of a matrix *trans*-butene/NO_2/Ar = 2.5/1/400 at 390 mW cm^{-2} for 1 h. Two new bands are readily detected, one at 1646 cm^{-1}, the other at 755 cm^{-1}. Three additional, much weaker new bands are found at 1367, 1035, and 921 cm^{-1}. These are more easily observed upon 590-nm irradiation of the more concentrated 2.5/1/100 matrix. Table II shows that all five bands exhibit identical absorbance growth behavior (columns 5 and 6), suggesting assignment to a single species. Isotopic shifts of the five product bands obtained by inducing reaction of *trans*-2-butene with $N^{16}O^{18}O$ and $N^{18}O_2$ are displayed in Table II, columns 1–4, and Figure 2 shows the ^{18}O isotope splitting of a band in the spectral range where we expect C–O stretching modes to absorb.

While no intensity changes were noticed in the absence of exposure of the matrix to visible light, the five new absorptions, after reaching a maximum, decreased upon continued irradiation at 590 nm. This is illustrated in Figure 1b by the difference of infrared spectra taken after 4 and 5 h of irradiation of a matrix *trans*-2-butene/NO_2/Ar = 2.5/1/100. The intensity ratios among all five decreasing bands remained constant over the entire photolysis period, a finding that is important since some bands, like those at 1646 and 755 cm^{-1}, overlap strongly with N_2O_4 ab-

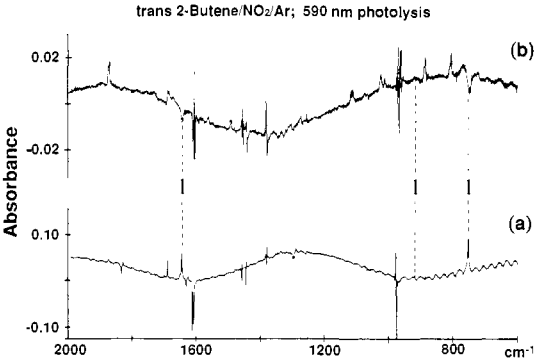

Figure 1. (a) Growth of absorptions in the spectral region 2000–600 cm^{-1} after the 1-h irradiation of a matrix *trans*-2-butene/NO_2/Ar = 2.5/1/400 at 590 nm and (b) absorption changes occurring between the fourth and fifth hour of 590-nm irradiation of a matrix *trans*-2-butene/NO_2/Ar = 2.5/1/100. Decreasing intermediate bands are marked as I. Other decreasing bands are due to *trans*-2-butene·NO_2 reactant depletion (1609 (NO_2), 1456, 1442, 1380, 1066, 975, and 967 (butene) cm^{-1}. Increasing bands are those of *trans*-2-butene oxide (Table III) and N_xO_y isomerization (Table I).

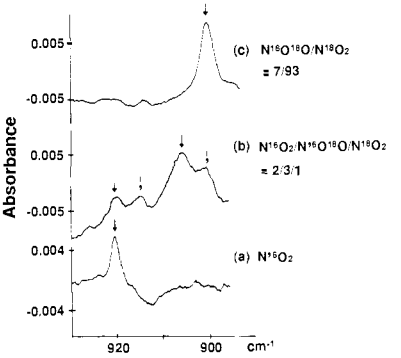

Figure 2. ^{18}O isotope effect on the 921-cm^{-1} absorption of the trapped intermediate (see Table II). (a) *trans*-butene/NO_2/Ar = 2.5/1/400, with $N^{16}O_2$, (b) *trans*-butene/NO_2/Ar = 2.5/1/100, with $N^{16}O_2$/$N^{16}O^{18}O$/$N^{18}O_2$ = 2/3/1 (the 907-cm^{-1} band overlaps with an absorption of asymmetric N_2O_4 (Table I) but could readily be differentiated from the latter by its different growth behavior), and (c) *trans*-2-butene/NO_2/Ar = 2.5/1/100, with $N^{16}O^{18}O$/$N^{18}O_2$ = 7/93. Spectra were obtained by irradiation of matrices for 1 h at 590 nm, 390 mW cm^{-2}.

(6) McKean, D. C.; Mackenzie, M. W.; Morrison, A. R.; Lavalley, J. C.; Janin, A.; Fawcett, V.; Edwards, H. G. M. *Spectrochim. Acta* **1985**, *41A*, 435–450.
(7) Fateley, W. G.; Bent, H. A.; Crawford, B., Jr. *J. Chem. Phys.* **1959**, *31*, 204–217.
(8) Varetti, E. L.; Pimentel, G. C. *J. Chem. Phys.* **1971**, *55*, 3813–3821.
(9) Bandow, H.; Akimoto, H.; Akiyama, S.; Tezuka, T. *Chem. Phys. Lett.* **1984**, *111*, 496–500.
(10) Frei, H. Unpublished results.
(11) St. Louis, R. V.; Crawford, B., Jr. *J. Chem. Phys.* **1965**, *42*, 857–864.

Table II. Infrared Spectrum of Reaction Intermediates Observed in a Matrix *trans*-2-Butene/NO_2/Ar = 2.5/1/400

frequency, cm^{-1} [a]				absorbance growth		
$C_4H_8{}^{16}ON^{16}O$	$C_4H_8{}^{16}ON^{18}O$	$C_4H_8{}^{18}ON^{16}O$	$C_4H_8{}^{18}ON^{18}O$	A_1[b]	A_3	assignment
1645.5	1605.0	1644.2	1605.0	0.90	0.92	ν(N=O)
1366.7	1366.7	1366.7	1366.7	0.06	0.05	$\delta(CH_3)$
1035.0	1033.4	1031.8	1030.3	0.04	0.04	ν(C-C)
920.5	914.9	906.9	901.2	0.08	0.09	ν(C-O)
754.6	754.6	735.8	735.8	1.00	1.00	ν(O-N)

[a] Absorptions assigned to $C_4H_8{}^{16}ON^{18}O$, $C_4H_8{}^{18}ON^{16}O$, and $C_4H_8{}^{18}ON^{18}O$ on the basis of comparisons of band intensities of isotopically enriched NO_2 samples with different composition: *trans*-2-butene/NO_2/Ar = 2.5/1/400 with $N^{16}O_2/N^{16}O^{18}O/N^{18}O_2$ = 1/2/1, *trans*-2-butene/NO_2/Ar = 2.5/1/100 with $N^{16}O_2/N^{16}O^{18}O/N^{18}O_2$ = 2/3/1 and 0.1/7/93. [b] Peak absorbances A_t (t in hours), normalized to the absorbance at 755 cm^{-1}, observed upon 590-nm irradiation at 390 mW cm^{-2}.

Table III. Infrared Product Spectrum Assigned to *trans*-2-Butene Oxide in a Matrix of *trans*-2-Butene/NO_2/Ar = 2.5/1/100

frequency, cm^{-1}		absorbance growth	
C_4H_8O	$C_4H_8{}^{18}O$[a]	A_2[b]	A_3
2998	2999	c	c
2977	2980	c	c
2932	2935	c	c
2928	2927	c	c
1492	1487	0.35	0.36
1460	1459	0.44[c]	0.41[c]
1383	1383	1.38[c]	1.43[c]
1157	1155	0.09	0.10
1118	1114	0.50	0.48
1113	1113	0.47	0.47
1026	1026	0.76	0.77
1015	1015	0.48	0.50
958	958	0.25	0.26
891	877	1.00	1.00
812	804	0.89	0.90
726	721	0.35	0.34
471	458	0.38	0.36

[a] Observed in matrices containing ^{18}O enriched NO_2 of composition $N^{16}O^{18}O/N^{18}O_2$ = 7/93 and $N^{16}O_2/N^{16}O^{18}O/N^{18}O_2$ = 2/3/1. [b] Peak absorbances A_t (t in hours), normalized to the absorbance at 891 cm^{-1}, observed upon 590-nm irradiation at 405 mW cm^{-2}. [c] Band overlaps with *trans*-2-butene absorption.

sorptions. It confirms the assignment to a single species, apparently a trapped reaction intermediate.

At the same time, a set of new infrared absorptions grew in (Figure 1b). All these bands are listed in Table III except for the one at 1872 cm^{-1}, which is readily assigned to NO[7]. Columns 3 and 4 of the table show that all new absorptions grow at constant relative intensities, consistent with assignment to a single reaction product. The spectrum displayed in Table III agrees completely with that of *trans*-2-butene oxide reported in the gas phase[12] and Ar matrix.[13] ^{18}O isotope shifts of the product bands, obtained by 590 nm irradiation of matrices *trans*-2-butene/NO_2/Ar = 2.5/1/100 with isotopic compositions $N^{16}O_2/N^{16}O^{18}O/N^{18}O_2$ = 0.1/7/93 and 2/3/1 are also shown in Table III. The cumulative ^{18}O shift measured is 1.066, consistent with the presence of one oxygen in the product. Assignment of the 1872 cm^{-1} band to NO is confirmed by the observation of its 1823-cm^{-1} ^{18}O counterpart.

No other trapped intermediate or final product bands were found upon irradiation at any of the red, yellow, or green wavelengths (613, 590, 573, and 514 nm). In particular, no absorptions of *cis*-2-butene oxide appeared. The latter has an intense band at 1102 cm^{-1},[13,14] whose extinction coefficient, according to gas-phase spectra, is about the same as that of the 1118 cm^{-1} band of *trans*-2-butene oxide.[12] In our most intense infrared product spectrum, obtained by 21-h irradiation of a matrix *trans*-butene/NO_2/Ar = 2.5/1/100 at 590 nm, an absorbance of 0.135 was measured for the 1118-cm^{-1} *trans*-2-butene oxide band, while the same spectrum showed at 1102 cm^{-1} a peak to peak noise of 0.0025 absorbance unit. This puts a lower limit of 50 on the *trans*-2-butene to *cis*-2-butene oxide product branching ratio.

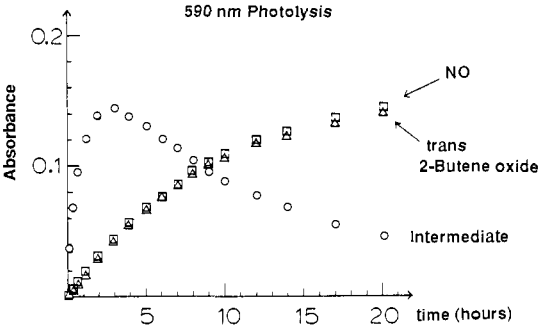

Figure 3. Absorbance growth of trapped intermediate (755 cm^{-1}), *trans*-2-butene oxide (812 cm^{-1}), and NO (1872 cm^{-1}) upon prolonged irradiation of a matrix *trans*-2-butene/NO_2/Ar = 2.5/1/100 at 590 nm, 400 mW cm^{-2}.

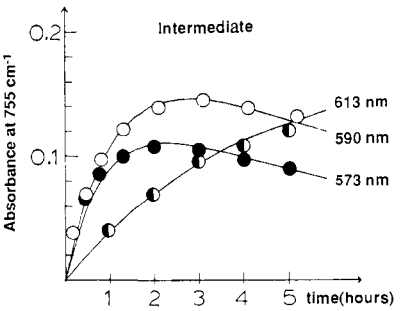

Figure 4. Absorbance growth behavior of trapped intermediate band at 755 cm^{-1} upon irradiation of matrices *trans*-2-butene/NO_2/Ar = 2.5/1/100 at 613 nm (299 mW cm^{-2}), 590 nm (405 mW cm^{-2}), and 573 nm (242 mW cm^{-2}). Each curve has been obtained starting with a new matrix. Solid traces represent fits of equations 5′ and 6′ to I and P absorbance growth at the respective photolysis wavelengths.

3. Growth Kinetics and Laser-Power Dependence. In order to elucidate the mechanism of the photoinduced reaction and to determine the wavelength dependence of yields, the kinetic behavior of trapped intermediate and product absorptions was measured as function of photolysis wavelength and laser power. Measured bandwidths were found to be constant, within uncertainties, over the entire photolysis period, which allowed us to use peak absorbances in place of integrated absorbances.

Figure 3 shows the kinetics of infrared bands of the trapped intermediate (755 cm^{-1}) and the final products *trans*-2-butene oxide (812 cm^{-1}) and NO (1872 cm^{-1}) upon prolonged 590-nm irradiation at 400 mW cm^{-2}. The intermediate exhibits growth and decay typical for a species that is being photolyzed itself, to *trans*-2-butene oxide and NO according to the spectroscopic evidence presented in the preceding section.

The photolysis-wavelength dependence of the absorbance growth of the trapped intermediate with red and yellow photons is displayed in Figure 4 (matrix concentration: *trans*-butene/NO_2/Ar = 2.5/1/100). Both the rate of formation and that of subsequent photolysis increase with decreasing photolysis wavelength, leading

(12) Kirchner, H. H. *Z. Phys. Chem. N. F.* **1963**, *39*, 273–305.
(13) Kuehne, H.; Forster, M.; Hulliger, J.; Ruprecht, H.; Bauder, A.; Gunthard, H. H. *Helv. Chim. Acta* **1980**, *63*, 1971–1999.
(14) Nakata, M.; Frei, H. *J. Phys. Chem.* Submitted for publication.

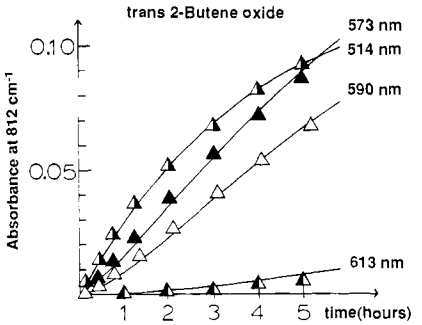

Figure 5. Growth of *trans*-2-butene oxide absorption at 812 cm^{-1} measured in the experiment described in the caption of Figure 4, and a photolysis experiment at 514 nm (49 mW cm^{-2}). Solid traces represent fits of equations 5′ and 6′ to I and P absorbance growth at the respective photolysis wavelengths.

Scheme I

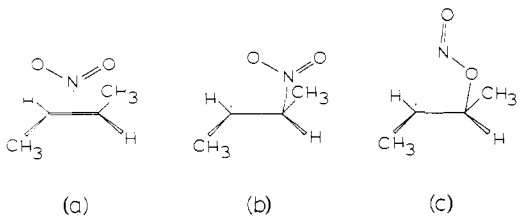

to a rapid decrease of the attainable maximum intermediate buildup. Upon 514-nm green-light irradiation, at laser intensities as low as 50 mW cm^{-2}, even the most intense intermediate bands can barely be observed.

Figure 5 shows the *trans*-2-butene oxide growth in the same series of experiments as presented in Figure 4. The absorbance growth upon 613-nm irradiation exhibits a clear induction period, consistent with production by secondary photolysis of the reaction intermediate. Sigmoidal growth behavior is observed in the 590-nm irradiation experiment, and, though less distinct, upon 573-nm photolysis. When photolyzing at 514 nm, however, no sigmodial behavior can be discerned even at very low laser intensity. At all photolysis wavelengths, NO exhibits a growth behavior identical with that of *trans*-2-butene oxide. The growth of the trapped reaction intermediate was found to depend linearly on the photolysis laser power at all irradiation wavelengths and matrix concentrations. *trans*-2-Butene oxide and NO exhibit a close to linear dependence on photolysis laser power upon irradiation at 514 nm.

IV. Discussion

1. Identification of the Trapped Intermediate. Two findings point to the molecular formula $C_4H_8O_2N$ for the trapped intermediate. First, prolonged irradiation of a matrix *trans*-2-butene/NO_2/Ar = 2.5/1/100 led to 15 ± 2% depletion of *trans*-butene reactant absorptions. For a statistical distribution of the solute among substitutional matrix sites, we calculate that 14% of all butenes have one NO_2 nearest neighbor, and that the abundance of higher butene–NO_2 aggregates lies below 4%. This result implies that the observed photochemistry originates from reaction of one NO_2 with one butene molecule. Second, the photolysis products of the intermediate are C_4H_8O and NO, consistent with the molecular formula $C_4H_8O_2N$ for the trapped intermediate.

The five infrared bands of the trapped intermediate, Table II, allow us to decide among three possible structures shown in Scheme I, namely a butene–NO_2 complex (a), a nitro butyl radical (b), and a butyl nitrite radical (c). While the two most intense bands of the intermediate at 1646 and 755 cm^{-1} lie close to the asymmetric stretching and bending modes of isolated NO_2 (1611 and 755 cm^{-1}), the observed ^{18}O isotope shifts of the 1646-cm^{-1} band are inconsistent with mere formation of a complex. For the monolabeled intermediate, two bands with shifts of 1.3 and 40.5 cm^{-1} are observed, while the asymmetric stretch of $N^{16}O^{18}O$ is

Scheme II

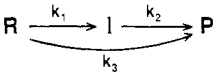

R : trans 2-butene·NO_2 reactant pair

I : nitrite radical intermediate

P : trans 2-butene oxide·NO product pair

shifted by only 16 cm^{-1} relative to the absorption of the $N^{16}O_2$ species. Moreover, observation of two bands with large ^{18}O shifts below 1000 cm^{-1}, namely at 921 and 755 cm^{-1}, definitively rules out complex a since the only NO_2 infrared absorption in that part of the spectrum would be the bending mode around 750 cm^{-1}.

The 4-fold splitting of the 920-cm^{-1} intermediate absorption observed when using a $N^{16}O_2/N^{16}O^{18}O/N^{18}O_2$ isotope reactant mixture allows us to decide among nitro structure b and nitrite form c. Only the nitrite with its inequivalent oxygens is expected to split into four bands (one originating from $C_4H_8{}^{16}O_2N$, two from $C_4H_8{}^{16}O^{18}ON$, and one from $C_4H_8{}^{18}O_2N$). In the case of the nitro form or other possible structures with equivalent oxygens like a five-membered ring, $\overbrace{CCONO}$,[15] the 921-cm^{-1} absorption would give rise to only three split bands. Structure b is further ruled out by the absence of two intense bands around 1550 and 1350 cm^{-1} with substantial ^{18}O shifts, characteristic for the asymmetric and symmetric stretching modes of the nitro group.[16]

Additional spectral observations strongly support structure c. For example, the 1646 cm^{-1} band is exactly where the N=O stretching mode of the trans form (with respect to the NO single bond) of a butyl nitrite molecule absorbs[16] (1638 cm^{-1} in the case of *trans-tert*-butyl nitrite, isolated in solid Ar;[17] cis (N–O) forms have a ν(N=O) absorption at significantly lower frequency, in the range 1625–1605 cm^{-1}).[16] Furthermore, the observed ^{18}O shifts of the 1646-cm^{-1} band for the monosubstituted intermediate of 1.3 and 40.5 cm^{-1} (Table II) are identical with those reported for the ν(N=O) absorption of ^{18}O monosubstituted *trans*-methyl nitrite.[18] The 755-cm^{-1} intermediate absorption agrees both in frequency and in terms of its ^{18}O shift with a NO single bond stretching mode of nitrites.[16] The 14 cm^{-1} ($C_4H_8{}^{18}ON^{16}O$) and 19 cm^{-1} ($C_4H_8{}^{18}ON^{18}O$) shifts of the 921-cm^{-1} band suggest that this mode contains a strong C–O stretching contribution. We conclude that the reaction intermediate is the butyl nitrite radical (c) with trans conformation with respect to the N–O bond. The work presented in this paper alone does not allow us to draw a conclusion about the conformation with respect to the central CC bond. However, evidence from our study of the photoinduced *cis*-2-butene + NO_2 reaction suggests that the 2-butyl nitrite radical whose spectrum is given in Table II has a trans carbon skeleton.[14]

2. Reaction Kinetics. The growth of the nitrite radical depends linearly on laser power at all photolysis wavelengths and matrix concentrations used, hence it is always produced by a one-photon event. The situation with regard to the final reaction products *trans*-2-butene oxide and NO is more complicated. While the close to linear dependence of the *trans*-2-butene oxide growth upon 514-nm photolysis of *trans*-2-butene·NO_2 pairs suggests that a substantial contribution to its production originates from a direct, single-photon path, spectrum Figure 1b shows that upon irradiation at 590 nm *trans*-2-butene oxide is also produced by secondary photolysis of the trapped nitrite radical intermediate. This is consistent with the observation of an induction period of the *trans*-2-butene oxide absorbance growth when exciting with red or yellow photons (Figure 5). Hence, *trans*-2-butene oxide and

(15) Charlton, J. L.; Liao, C. C.; deMayo, P. *J. Am. Chem. Soc.* **1971**, *93*, 2463–2471.

(16) (a) Tarte, P. *J. Chem. Phys.* **1952**, *20*, 1570–1575. (b) Colthrup, N. B.; Daly, L. H.; Wiberley, S. E. *Introduction to Infrared and Raman Spectroscopy*; Academic Press: New York, 1975; pp 328–330.

(17) Barnes, A. J.; Hallam, H. E.; Waring, S.; Armstrong, J. R. *J. Chem. Soc., Faraday Trans. 2* **1976**, *72*, 1–10.

(18) Ghosh, P. N.; Gunthard, Hs. H. *Spectrochim. Acta* **1981**, *37A*, 1055–1065.

Table IV. Photolysis-Wavelength Dependence of Initial Slopes of Growth Curves (*trans*-2-Butene/NO_2/Ar = 2.5/1/100)[a]

λ, nm	$\frac{(dA^1(\lambda)/dt)_0}{(dA^1(590)/dt)_0} = \frac{k_1(\lambda)}{k_1(590)}$	$\frac{(dA^P(\lambda)/dt)_0}{(dA^P(590)/dt)_0} = \frac{k_3(\lambda)}{k_3(590)}$
613	0.31	0.0
590	(1.0)	(1.0)
573	1.8	3.1
514	7.4	38

[a] Slopes normalized to laser photon intensity of 2×10^{-6} mol cm^{-2} s^{-1} used in the 590-nm irradiation experiment.

NO are produced along two reaction paths, namely along a direct, one-photon path from *trans*-2-butene and NO_2, which is most pronounced at high photon energies, and along a two-photon path via secondary photolysis of the trapped nitrite radical intermediate, dominating at long photolysis wavelengths. This leads us to the kinetic Scheme II.

Starting with a fixed reservoir of *trans*-2-butene–NO_2 pairs, the kinetic behavior of reactants, intermediate, and products according to Scheme II is described by the following set of differential equations (in terms of concentrations)

$$\frac{d[R]}{dt} = -k_1[R] - k_3[R] \quad (1)$$

$$\frac{d[I]}{dt} = k_1[R] - k_2[I] \quad (2)$$

$$\frac{d[P]}{dt} = k_2[I] + k_3[R] \quad (3)$$

with $k_1 = \epsilon_{vis}^{NO_2} \cdot \phi_1 \cdot I$, $k_2 = \epsilon_{vis}^{I} \cdot \phi_2 \cdot I$, and $k_3 = \epsilon_{vis}^{NO_2} \cdot \phi_3 \cdot I$ ($\epsilon_{vis}^{NO_2}$, ϵ_{vis}^{I} are decadic extinction coefficients of NO_2 and nitrite radical intermediate, respectively, at visible photolysis wavelength; ϕ is the reaction quantum efficiency; I is the laser photon intensity). These expressions for the rate constants hold in the weak absorption limit, which in our experiments applies both for the case of NO_2 and the nitrite radical.

Equations 1–3 allow us to make an initial estimate of the photolysis-wavelength dependence of the rate constants k_1 and k_3 on the basis of the slopes of nitrite radical and *trans*-2-butene oxide absorbance growths at the beginning of photolysis. The concentration of nitrite radicals before photolysis, $[I]_0$, is zero, hence $(d[I]/dt)_0 = k_1[R]_0$ and $(d[P]/dt)_0 = k_3[R]_0$. These relations expressed in terms of experimentally measured absorbances are

$$(dA^I/dt)_0 = k_1 A_0^R \epsilon^I/\epsilon^R$$

$$(dA^P/dt)_0 = k_3 A_0^R \epsilon^P/\epsilon^R$$

(A_0^R is the reactant pair absorbance before photolysis; ϵ^R, ϵ^I, ϵ^P are the extinction coefficients of reactant, intermediate, and product infrared absorptions, respectively). The two equations show that if the nitrite radical and *trans*-2-butene oxide growth curves obtained at the various photolysis wavelengths were scaled to the same initial reactant pair absorbance, a comparison of the initial slopes of the absorbance growth curves would yield the photolysis wavelength dependence of k_1 and k_3, respectively. The result is shown in Table IV. The data indicate a rapid increase, with increasing laser photon energy, of both the rate constant of intermediate formation, k_1, and that of direct, one-photon photolysis of *trans*-2-butene–NO_2 pairs to *trans*-butene oxide and NO, k_3. The table also shows that the latter increases considerably more steeply with photon energy than the former.

A more accurate way to obtain the laser-photolysis-wavelength dependence of k_1 and k_3 in the red and yellow spectral range and to determine the rate constant k_2 is to fit the integrated rate laws to the nitrite radical and *trans*-2-butene oxide (or NO) absorbance growth curves shown in Figures 4 and 5. Integration of the differential equations 1–3, using the integrating factor method in the case of eq 2[19] gives

$$[R] = [R]_0 e^{-(k_1+k_3)t} \quad (4)$$

$$[I] = \frac{[R]_0 k_1}{k_2 - (k_1 + k_3)}(e^{-(k_1+k_3)t} - e^{-k_2 t}) \quad (5)$$

$$[P] = [R]_0\left(1 + \frac{1}{k_2-(k_1 + k_3)}[k_1 e^{-k_2 t} - (k_2 - k_3)e^{-(k_1+k_3)t}]\right) \quad (6)$$

Expressed in absorbances

$$A^R = A_0^R e^{-(k_1+k_3)t} \quad (4')$$

$$A^I = A_\infty^P \frac{\epsilon^I}{\epsilon^P} \frac{k_1}{k_2 - (k_1 + k_3)}(e^{-(k_1+k_3)t} - e^{-k_2 t}) \quad (5')$$

$$A^P = A_\infty^P\left(1 + \frac{1}{k_2 - (k_1 + k_3)}[k_1 e^{-k_2 t} - (k_2 - k_3)e^{-(k_1+k_3)t}]\right) \quad (6')$$

Fits of eq 5′ and 6′ to the nitrite radical intermediate and to the *trans*-2-butene oxide absorbance growth, respectively, using iterative approximation by the Gauss–Newton procedure[20] are shown for each laser-irradiation experiment as solid curves in Figures 4 and 5. NO_2 or *trans*-2-butene infrared absorbance decays (eq 4′) were not used for parameter fitting since reactant pair absorptions were overlapped by much more intense absorptions of isolated species, adding large uncertainities to absorbance difference measurements. Values for the four parameters k_1, k_2, k_3, and A_∞^P and the asymptotic absorbance growth of the 812-cm^{-1} trans-2-butene oxide band are given in Table V. The ratio ϵ^I/ϵ^P of the extinction coefficients of the 755-cm^{-1} nitrite radical and the 812-cm^{-1} *trans*-2-butene oxide infrared bands was determined experimentally as 10. The measurement involved accumulation of nitrite radical intermediate by prolonged irradiation at a red wavelength, followed by 2-min photolysis at 514 nm. Green-light irradiation over such a brief period resulted in almost exclusive formation of *trans*-2-butene oxide by decomposition of the nitrite radical, with very little growth originating from direct photolysis of *trans*-butene–NO_2 pairs. Therefore, the extinction coefficient ratio ϵ^I/ϵ^P could be directly determined by measuring the absorbance changes of the 755-cm^{-1} and the 812-cm^{-1} bands. In contrast to the absorbance growth curves of *trans*-2-butene oxide obtained upon photolysis with red or yellow light, the 514-nm curve exhibits no sigmoidal behavior and fits a single exponential function well. Due to efficient secondary photolysis of the butyl nitrite radical at this wavelength, even its strongest absorption at 1646 and 755 cm^{-1} were barely observable. Hence, the steady-state approximation was employed, and the sum $k_1 + k_3$ was determined from the resulting equation $[P] = [R]_0(1 - \exp[-(k_1 + k_3)\cdot t])$. A crude estimate of separate values for k_1 and k_3 at 514 nm, based on the wavelength dependence of k_1 and k_3 obtained from initial slopes (Table IV) and the 590-nm values of k_1 and k_3 (Table V), suggests that they lie within the same order of magnitude.

Rows 5–8 of Table V exhibit the first-order rate constants normalized to the laser photon intensity used in the 590-nm irradiation experiment, 2×10^{-6} mol cm^{-2} s^{-1}. Ratios of these normalized rate constants give relative values of the products of extinction coefficient and reaction quantum efficiency, $\epsilon\phi$. Clearly, all normalized rate constants increase with decreasing photolysis wavelength, confirming for k_1 and k_3 the trend predicted by the initial slopes (Table IV). Moreover, the rate constants of Table V confirm the much more rapid increase of k_3, with decreasing photolysis wavelength, already apparent from the data of Table IV.

3. Reaction Mechanism. The wavelength dependence of the kinetics allows us to address key mechanistic points like the reacting state of NO_2 and the control of the branching between the

(19) Smirnov, W. I. *Lehrgang der hoheren Mathematik*, Part II; VEB Deutscher Verlag der Wissenschaften: Berlin, 1964; p 211.
(20) Walsh, G. R. *Methods of Optimization*; Wiley: New York, 1975.

Table V. Photolysis-Wavelength Dependence of First-Order Rate Constants Obtained from Integrated Equations (*trans*-2-Butene/NO_2/Ar = 2.5/1/100)

		adjusted parameters					
λ, nm	power, mW cm^{-2}	k_1, h^{-1}	k_2, h^{-1}	k_3, h^{-1}	A_∞^P [a]	k_t, h^{-1}	$\phi_t(\lambda)/\phi_t(613)$
613	299	0.02 ± 0.01	0.21 ± 0.04	0.00 ± 0.01	0.21 ± 0.05		
590	405	0.09 ± 0.02	0.90 ± 0.18	0.02 ± 0.02	0.20 ± 0.05		
573	242	0.07 ± 0.02	1.13 ± 0.23	0.04 ± 0.02	0.23 ± 0.05		
514	49	*b*	*b*	0.27 ± 0.03[b]	0.12 ± 0.03		
				Normalized Values[c]			
613		0.03 ± 0.01	0.28 ± 0.05	0.00 ± 0.01		0.03	(1.0)
590		0.09 ± 0.02	0.90 ± 0.18	0.02 ± 0.02		0.11	1.8
573		0.12 ± 0.03	1.95 ± 0.40	0.07 ± 0.03		0.19	2.4
514				2.60 ± 0.28[b]		2.60[b]	12

[a] Asymptotic absorbance of the 812-cm^{-1} *trans*-2-butene oxide band. [b] Steady-state approximation; only $k_1 + k_3$ could be determined (see the text). [c] Rate constants normalized to the laser photon intensity of 2×10^{-6} mol cm^{-2} s^{-1} used in the 590-nm irradiation experiment.

Scheme III

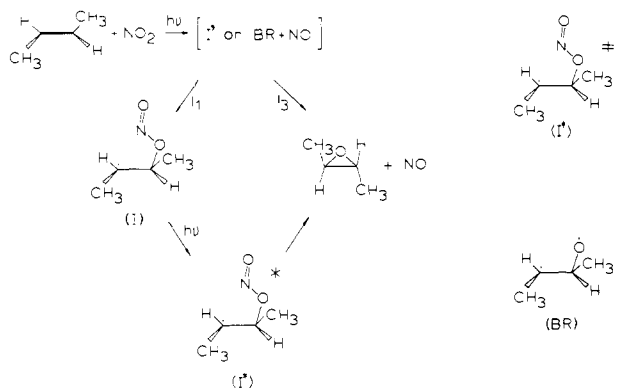

observed products, butyl nitrite radical and epoxide + NO. A particularly interesting question is that regarding the origin of the observed stereochemical retention. Observation of a correlation between the stereochemistry of epoxide and trapped butyl nitrite radical in the case of the red-light induced *cis*-2-butene + NO_2 reaction[14] strongly suggests involvement of a transient precursor. Therefore, we will restrict the discussion of possible mechanisms to the two precursors we can conceive of, a hot nitrite radical and an oxirane biradical, respectively. The two corresponding paths are depicted in Scheme III, and will be discussed in turn.

i. **Hot Nitrite Radical Path.** Reaction of NO_2 with a nearest neighbor *trans*-2-butene molecule is initiated by $^2B_2 \leftarrow \tilde{X}^2A_1$ excitation of NO_2 by absorption of a red, yellow, or green photon.[21] The excited NO_2 may add to the alkene double bond to form a vibrationally hot, electronic ground-state butyl nitrite radical intermediate, labeled I* in Scheme III. I* would act as a precursor of both the trapped butyl nitrite radical and *trans*-2-butene oxide, depending on whether it is stabilized by transfer of its excess vibrational energy to the surrounding matrix or whether it undergoes elimination of NO. Using known standard enthalpies of formation for NO_2 and *trans*-2-butene of 7.9 and −2.67 kcal, respectively,[22] and an estimated standard enthalpy of formation of 6 kcal for the (ground state) butyl nitrite radical (see Appendix), we find that the reaction of NO_2 + *trans*-2-butene → butyl nitrite radical is approximately thermoneutral. Therefore, the intermediate would carry a maximum vibrational energy equal to the energy of the photon initially absorbed by NO_2, i.e. 47 kcal at 613 nm and 56 kcal at 514 nm. If we take the average N–O bond energy of 48 kcal mol^{-1} [23] as an estimate for the upper limit of the barrier to NO elimination, we find that it lies no higher than, and probably close to, the maximum energy available to the intermediate. (Alternatively, one could take the approximate $\Delta H°$ of 40 kcal of reaction 8, to be discussed below, as an estimate for the upper limit of the NO elimination barrier). Therefore, production of epoxide via elimination of nitric oxide from a hot nitrite radical intermediate is possible. $\Delta H_f°(NO)$ = 21.6 kcal mol^{-1} [22] and estimated formation enthalpies of 6 and −30 kcal for butyl nitrite radical and *trans*-2-butene oxide, respectively (the Appendix), give $\Delta H°$ = −14 kcal mol^{-1} for the reaction step butyl nitrite radical → *trans*-2-butene oxide + NO. Hence, the overall reaction is only modestly exothermic. Electronic excitation of stabilized butyl nitrite radical by a (second) photon (Scheme III, I*) also results in elimination of NO, again giving exclusively the trans diastereomer of 2-butene oxide.

The sum k_t of the normalized rate constants k_1 and k_3 increases monotonically with decreasing photolysis wavelength, namely from 613 to 590 nm by a factor of 3.6, to 573 nm by a factor of 6.3, and to 514 nm by a factor of 86 (Table V, second column from the right). Extinction coefficient ratios of the reactant NO_2 at these wavelengths, determined from visible absorption spectra of matrices NO_2/Ar = 1/50 and *trans*-2-butene/NO_2/Ar = 2.5/1/50, are $\epsilon_{590}^{NO_2}/\epsilon_{613}^{NO_2}$ = 2.0, $\epsilon_{573}^{NO_2}/\epsilon_{613}^{NO_2}$ = 2.7, and $\epsilon_{514}^{NO_2}/\epsilon_{613}^{NO_2}$ = 7.5 (in suspensions of NO_2 and butene in solid Ar, no other absorptions were found in the red-green spectral range than those of the known $NO_2{}^2B_2 \leftarrow \tilde{X}^2A_1$ system reported in the literature[21,24]). Since the total rate constant, k_t, is proportional to the quantum efficiency $\phi_t = \phi_1 + \phi_3$ of *trans*-2-butene–NO_2 photolysis, $k_t = \phi_t(\lambda)\epsilon_\lambda^{NO_2}I$, the ratios $(k_t(\lambda)/k_t(613))/(\epsilon_\lambda^{NO_2}/\epsilon_{613}^{NO_2})$ give the photon-energy dependence of the *trans*-butene + NO_2 reaction quantum efficiency, $\phi_t(\lambda)/\phi_t(613)$. According to the last column of Table V, the efficiency increases very sharply, e.g. by a factor of 12 between 613 and 514 nm. Independent of the nature of the reaction intermediate, the steep increase of the *trans*-2-butene + NO_2 reaction quantum efficiency with photolysis photon energy indicates that the reacting NO_2 is vibrationally unrelaxed. In particular, it rules out the possibility that NO_2 relaxes to the ground vibrational level of the excited $^2B_2$ state around 12000 cm^{-1} [21,25] before reaction occurs. In such a case ϕ_t would not exhibit the observed dependence on photolysis wavelength. This finding is no surprise in view of the spectroscopically well-established fact that $NO_2{}^2B_2$ and high-lying $\tilde{X}^2A_1$ vibrational levels are heavily mixed (ref 21 and references therein), which makes it very unlikely that vibrational cascading within $^2B_2$ can compete with crossing over to the ground state. Given the unusually strong coupling between $^2B_2$ and $^2A_1$ levels, the most reasonable assumption we can make is that, upon photoexcitation, isoenergetic levels of the two states are populated according to their relative level density,[27] and that the proposed nitrite radical intermediate is born in its electronic ground state.

The most immediate explanation to propose for the observed increase of the reaction quantum efficiency with increasing photolysis photon energy would be RRK behavior, i.e. $\phi_t(\lambda)$ would

(21) Hsu, D. K.; Monts, D. L.; Zare, R. N. *Spectral Atlas of Nitrogen Dioxide*, Academic Press: New York, 1978.
(22) Benson, S. W.; Cruickshank, F. R.; Golden, D. M.; Haugen, G. R.; O'Neal, H. E.; Rodgers, A. S.; Shaw, R.; Walsh, R. *Chem. Rev.* **1969**, *69*, 279–324.
(23) Cotton, F. A.; Wilkinson, G. *Advanced Inorganic Chemistry*; Wiley: New York, 1962; p 88.
(24) Bolduan, F.; Jodl, H. J. *J. Mol. Struct.* **1984**, *116*, 361–375.
(25) There is recent evidence suggesting that T_0 of $^2B_2 \leftarrow \tilde{X}^2A_1$ may lie considerably lower, around 9800 cm^{-1}. See ref 24 and 26.
(26) Merer, A. J.; Hallin, K. E. *Can. J. Phys.* **1978**, *56*, 838–849.
(27) Schwartz, S. E.; Johnston, H. S. *J. Chem. Phys.* **1969**, *51*, 1286–1302.

reflect the increased energy of *trans*-2-butene–NO_2 pairs above the barrier to reaction with decreasing photolysis wavelength. The rise of ϕ_t in the range 613–514 nm appears too steep, however, to be explained by the statistical theory alone if the hot nitrite radical were the initial species produced by the NO_2 + *trans*-2-butene reaction. Assuming for the free radical addition NO_2 + alkene a barrier no higher than 20 kcal mol^{-1}, we predict that photons in the 613–514 nm range excite NO_2 to a narrow, 9 kcal energy range between 26 (613 nm) and 35 kcal (514 nm) above the barrier. The 12-fold increase of the reaction quantum efficiency from 613 to 514 nm seems large from an RRK standpoint for such a small energy range so high above the critical energy.[28] However, the rapidly growing $^2B_2$ level density relative to that of $\tilde{X}^2A_1$, i.e. the growing $^2B_2$ character of excited NO_2 with increasing photon energy may furnish an explanation. In the $^2B_2$ state NO_2 has less electron density on the oxygen atoms than in the $^2A_1$ state.[29] This makes $NO_2(^2B_2)$ a better electrophile toward attack on the C=C bond to form a C–O bond than the ground-state molecule. Therefore, we would expect the reactivity to go up with increasing $^2B_2$ character, hence decreasing photolysis wavelength, as observed.

The branching between trapped nitrite radical and epoxide + NO would be determined by the fate of the vibrationally hot, electronic ground state butyl nitrite intermediate ($I^\ddagger$). Insight into the product branching can be gained by considering the wavelength dependence of the ratio k_3/k_t. Using the steady-state expression for the concentration of $I^\ddagger$, one can readily show that this ratio is equal to the quantum efficiency to NO elimination from the hot intermediate (l_1 and l_3 stand for excitation-wavelength dependent, effective rate constants for stabilization of $I^\ddagger$ and elimination of NO, respectively (Scheme III)):

$$\frac{k_3}{k_t} = \frac{l_3}{l_1 + l_3} \tag{7}$$

According to the rate constants given in Table V, this ratio increases sharply with increasing photolysis photon energy over a relatively narrow wavelength range, from 0 at 613 nm to 0.18 at 590 nm and to 0.37 at 573 nm. According to our estimate of the barrier to NO elimination (see above), excitation of NO_2 with red or yellow photons would produce a nitrite radical intermediate with only modest excess energy available for fragmentation. Hence, this steep increase of the efficiency to NO elimination, from 0 to 37% over an energy range of just 3.3 kcal (from 613 to 573 nm), would be what we expect in the case of RRK behavior, since this range would lie right above the critical energy where reaction rate constants increase most sharply.[28] The implication would be that fragmentation of the hot, ground-state butyl nitrite radical occurs at a point where it still carries essentially all of the initial energy of the photoexcited NO_2. However, the observed stereochemical retention in the product would require that on the time scale of fragmentation, randomization of the energy in the hot butyl nitrite intermediate would not extend to the torsion around its central C–C bond, as will be discussed below.

ii. **Oxirane Biradical Path.** An alternative path to hot nitrite radical formation by NO_2 addition to the alkene would be oxygen atom transfer from the excited NO_2 to the C=C bond to give an oxirane biradical (labeled BR in Scheme III). An example of O atom transfer chemistry of NO_2 excited by visible light is the reaction with CO reported by Javan and co-workers.[30] Oxirane biradicals have been postulated as transient intermediates of the reaction of $O(^3P)$ with alkenes.[31,32] Product branching between epoxide and butyl nitrite radical would be determined by the competition between ring closure and trapping of the transient biradical by addition of the NO cage neighbor.

Taking an estimated $\Delta H°$ of −32 kcal mol^{-1} for

$$CH_2{=}CH_2 + O(^3P) \rightarrow \dot{C}H_2CH_2\dot{O}$$

as a guide[31] for the enthalpy change of the corresponding reaction of *trans*-2-butene, we arrive at an endothermicity of about 40 kcal for the reaction

$$\textit{trans}\text{-}CH_3CH{=}CHCH_3 + NO_2(\tilde{X}^2A_1) \rightarrow CH_3\dot{C}HCH(CH_3)O + NO \tag{8}$$

($D_0^0(NO_2)$ taken as 72 kcal mol^{-1} [33]). Allowing for a barrier of a few kcal for the reverse process 8, we arrive at an activation barrier for the forward reaction 8 that lies close to the observed reaction threshold for photoexcited NO_2 with *trans*-2-butene at 613 nm (47 kcal mol^{-1}). Therefore, if this biradical path were the correct mechanism, the observed steep increase of the reaction quantum efficiency ϕ_t with increasing photolysis photon energy (Table V) would be consistent with RRK behavior. This is different from the conclusion arrived at in the case of the hot nitrite radical path discussed before. According to the thermodynamic data presented in the preceding section, exothermicities for the reactions BR → epoxide, and BR + NO → butyl nitrite radical (I) would be around 54 and 40 kcal mol^{-1}, respectively.

As a sterically unhindered radical recombination, the trapping of the oxirane biradical by addition to a NO cage neighbor to form a butyl nitrite radical would most probably be a barrier-free process.[34] On the other hand, two CH_3, H eclipsed interactions are formed as the biradical closes to a ring, contributing an activation of about 3 kcal.[35] This would explain, in terms of RRK theory, the observed sharp increase of the ratio k_3/k_t with photolysis photon energy. The implication of the wavelength dependence of the product branching ratio is again that the intermediate, in this case the oxirane biradical, would undergo ring closure (or reaction with NO) at a moment where it still carries most of the excess kinetic energy supplied initially by photoexcited NO_2. Similar to the previously discussed mechanism, the stereochemical outcome of the reaction would suggest that the energy redistribution in the oxirane biradical would not involve the torsion around the central C–C bond.

The possibility of a direct O atom transfer from $NO_2(^2B_2)$ to butene to give *trans*-2-butene oxide without formation of an oxirane biradical intermediate, with butyl nitrite radical formed along a separate path, is very unlikely since it would be inconsistent with the observed correlation between the stereochemistry of the epoxide and the trapped butyl nitrite radical in the case of the *cis*-2-butene + NO_2 reaction,[14] as mentioned before.

iii. **Stereochemical Control.** Our observation of complete stereochemical retention in the epoxide product (no *cis*-2-butene oxide is formed) implies that internal rotation around the central C–C bond of the intermediate, be it the hot nitrite radical or the oxirane biradical, is slow on the scale of its lifetime. We expect the barrier to internal rotation about that bond for both proposed intermediates to be no more than a few kilocalories/mole, typical for internal rotation around a CC single bond (in the case of the oxirane biradical $\dot{C}H_2CH_2\dot{O}$ the barrier has been estimated to lie around 1 kcal mol^{-1} [31]). The matrix most probably does not affect the magnitude of this barrier substantially since in the cases where comparisons could be made the barrier to internal rotation of the matrix isolated molecule turned out to no more than 20–30% higher than that of the gas-phase species.[3]

If our assumption about barriers to ring closure and internal rotation around the central C–C are correct in the case of the oxirane biradical, they would be of similar magnitude. Hence, the complete lack of stereochemical scrambling would suggest that on the time scale of ring closure and addition of NO, redistribution of the excess energy of the BR does not encompass overtones of

(28) Robinson, P. J.; Holbrook, K. A. *Unimolecular Reactions*; Wiley: New York, 1972.
(29) Herzberg, G. *Electronic Spectra of Polyatomic Molecules*, Van Nostrand: New York, 1966; p 315.
(30) Herman, I. P.; Mariella, R. P., Jr.; Javan, A. *J. Chem. Phys.* **1978**, *68*, 1070.
(31) Cvetanovic, R. J.; Singleton, D. L. *Rev. Chem. Intermediates* **1984**, *5*, 183–226.
(32) Dupuis, M.; Wendoloski, J. J.; Takada, T.; Lester, W. A., Jr. *J. Chem. Phys.* **1982**, *76*, 481–487.
(33) Benson, S. W. *Thermochemical Kinetics*; Wiley: New York, 1968; pp 23–27.
(34) Gibian, M. J.; Corley, R. C. *Chem. Rev.* **1973**, *73*, 441–464.
(35) Lister, D. G.; McDonald, J. N.; Owen, N. L. *Internal Rotation and Inversion*; Academic Press: New York, 1978.

the torsion around the central C–C bond, as was pointed out earlier. This would not be too surprising in the light of the very short lifetime (psc) expected for the oxirane biradical because of the spin-allowed character of both ring closure and combination with NO (*trans*-2-butene + $NO_2(^2B_2)$ could give ^1BR + ^2NO in a spin-allowed reaction, followed by the spin conserving process $^1BR \rightarrow$ epoxide (S_0)).

In the case of the hot butyl nitrite radical path, the complete stereochemical retention would imply that the N–O bond breaks fast on the time scale of rotation around the butyl nitrite radical central C–C bond, despite the fact that the intermediate would carry about 50 kcal mol^{-1} of vibrational energy. Hence, a more severe lack of coupling of the initially excited stretch and bending vibrations of the hot butyl nitrite radical with high lying C–C torsional overtones would have to be invoked here in order to explain the observed complete stereospecificity.

The finding that epoxide along the two-photon path is also produced exclusively in the trans form cannot be explained yet in terms of a detailed energy path since we do not know at this point which excited electronic state(s) of the butyl nitrite radical are involved in the reaction (for example, whether direct photodissociation occurs upon excitation to a repulsive state or whether the intermediate photopredissociates from a bound state). Experiments are in progress to address this question.

V. Conclusions

This work demonstrates the potential of NO_2 as a reactant for controlled photooxidation of unsaturated hydrocarbons. In particular, it points to the advantage of using long-wavelength photons for accomplishing product specificity. First, it is interesting to note that no carbonyl compounds or product originating from fragmentation of the carbon skeleton are formed. Irrespective of which one of the two proposed transients is formed along the one-photon path (hot nitrite radical or oxirane biradical), a main factor that contributes to product control at this level is the low photon-excitation energy, coupled with the small reaction exothermicity. The result is deposition of insufficient kinetic energy in the transient and final oxidation product for opening up H or CH_3 group migration, though, in the case of the intermediate, there is just enough energy to permit subsequent reaction to give the epoxide. Sato and Cvetanovic found some time ago that upon gas-phase photoxidation of 1-butene by NO_2 excited around and above its 400-nm dissociation threshold, 1-butene oxide, *n*-butanal, methyl ethyl ketone, and products resulting from fragmentation of the carbon skeleton are formed.[36]

Regarding the stereochemical outcome, the complete retention of the trans configuration upon photooxidation is especially intriguing. Since the wavelength dependence of the product branching along the one-photon path (trapped nitrite radicals vs epoxide + NO) indicates that branching occurs from vibrationally unrelaxed intermediate, we attribute the stereochemical integrity to insufficient coupling of stretch and bending vibrations of the transient with torsion around its central C–C bond on the time scale of reaction to epoxide + NO and stabilization as butyl nitrite radical. Since this is an intramolecular property of the transient, we believe that the rare-gas environment has no marked influence on the product stereochemistry. This opens up the possibility of conducting the photooxidation in a higher temperature environment without loss of stereochemical integrity.

Acknowledgment. This work was supported by the Director, Office of Energy Research, Office of Basic Energy Sciences, Chemical Sciences Division, of the U.S. Department of Energy under Contract No. DE-AC03-76 SF00098. M.N. was supported by a grant from the Japan–US Cooperative Photoconversion and Photosynthesis Research Program. The authors thank a reviewer for valuable comments concerning the proposed mechanism.

Appendix

The enthalpy of formation of the butyl nitrite radical was determined by first calculating $\Delta H_f°$ of the (closed shell) *trans*-2-butyl nitrite $CH_3CH_2CH(CH_3)ONO$ by aid of Benson's additivity rules for thermochemical properties.[22,32] $\Delta H_f° = -37.2$ kcal mol^{-1} so obtained was then used to estimate $\Delta H_f°$ of $CH_3\dot{C}HCH(CH_3)ONO$ by subtracting from the former the enthalpy of formation of a H atom, $\Delta H_f°(H) = 52.1$ kcal mol^{-1},[22] and adding to it the dissociation energy of a C–H bond, 95.3 kcal mol^{-1},[22] giving $\Delta H_f°(I) = +6$ kcal mol^{-1}. The enthalpy of formation of *trans*-2-butene oxide was estimated at −30.3 kcal mol^{-1} using the same rules.

(36) Sato, S.; Cvetanovic, R. J. *Can. J. Chem.* **1958**, *36*, 279–281.